Triaxial tests of mortar and neat cement cylinders

Autor(en): **Sims, James R. / Krahl, Nat W. / Victory, S.P. Jr.**

Objekttyp: **Article**

Zeitschrift: **IABSE publications = Mémoires AIPC = IVBH Abhandlungen**

Band (Jahr): **26 (1966)**

PDF erstellt am: **26.09.2024**

Persistenter Link: https://doi.org/10.5169/seals-20892

Triaxial Tests of Mortar and Neat Cement Cylinders

Essais triaxiaux sur des éprouvettes cylindriques de mortier et de ciment pur

Dreiachsige Versuche an Zylinderproben aus Mörtel und reinem Zement

JAMES R. SIMS
Professor of Civil Engineering, Rice University, Houston, Texas

NAT W. KRAHL
Associate Professor of Structural Engineering, Rice University, Houston, Texas

S. P. VICTORY, Jr.
Project Engineer, Hudson Engineering Corporation, Houston, Texas

Introduction

No completely satisfactory quantitative theory of failure of concrete under combined stress is available. Recent structural applications have indicated a need for information on failure when a brittle material is loaded with a significantly high pore pressure in addition to the stresses arising from external load. One example of such an application is associated with the grouting of steel tubes in extremely deep bore-holes in the process of oil production from high pressure underground gas reservoirs. Recent development of a field termed "Rock Mechanics" in the United States indicates a broader importance. The aim of this investigation was to accumulate additional data on the behavior of mortar and neat cement under triaxial stress. Specifically, information was sought concerning the influence of confining pressure and pore pressure on the axial strength of cylindrical specimens and the accompanying stress-strain and volume change relationships.

The High-pressure Triaxial Test Cell

Fig. 1 shows a photograph of the high-pressure triaxial test cell mounted between the fixed and movable heads of a universal testing machine, and Fig. 2 shows a section through the test cell. The cell was designed for internal pressures up to 20,000 psi and is patterned after earlier equipment designed by GRIGGS [1]. In essence, the design of the cell allows a triaxial test to be performed on a small cylindrical specimen, one-half inch diameter by one inch long, with measurements of confining pressure, pore pressure, axial force, specimen axial deformation, and specimen volume change.

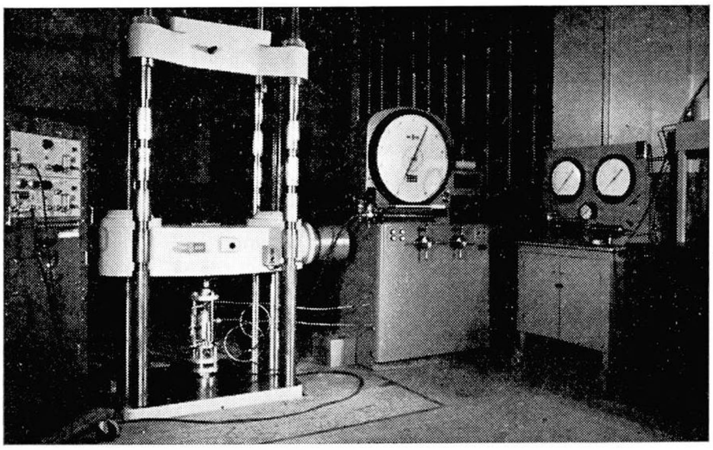

Fig. 1.

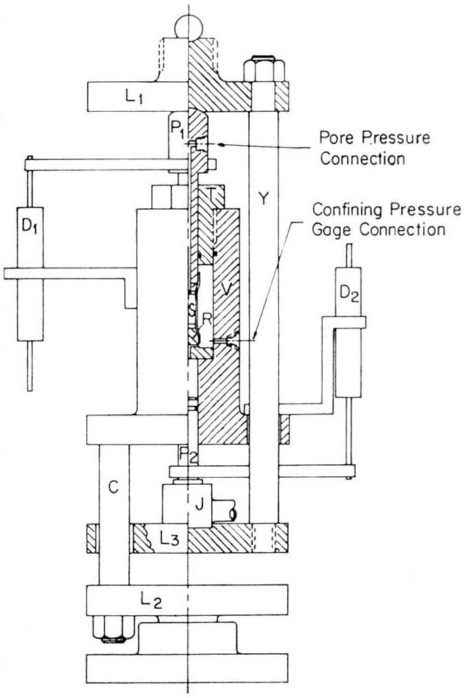

Fig. 2. Triaxial test apparatus.

Operation of the cell during a test can best be explained with reference to Fig. 2, which shows a specimen, S, mounted in the test chamber of the pressure vessel, V. The vessel is supported by three columns, C, from plate L_2 which bears on the fixed head of a testing machine. An hydraulic jack, J, rests on plate L_3 and activates piston P_2, generating a pressure within the liquid above. Specimens rest on stopper R, which contains a hole through which the liquid above Piston P_2 has access to the larger cavity around the specimen. Plate L_3 is suspended from plate L_1 by means of three columns, Y, and plate L_1 bears on upper piston P_1, which enters the pressure vessel through threaded plug T and bears on the upper end of the specimen assembly. Thus the jack controls the pressure in the test chamber and causes a hydrostatic pressure to be exerted upon all sides of the specimen. The pore pressure connection is made through a hole in the upper piston P_1. Axial force is introduced when the movable head of the testing machine bears on the spherical head at the center of plate L_1. Linear transformers D_1 and D_2 reflect the motion of both pistons relative to the vessel and the electrical output of the system is recorded. Proper calibration of the equipment allows the determination of specimen axial deformation and, for a jacketed specimen, volume change.

Fig. 3 shows a schematic diagram of the test facility.

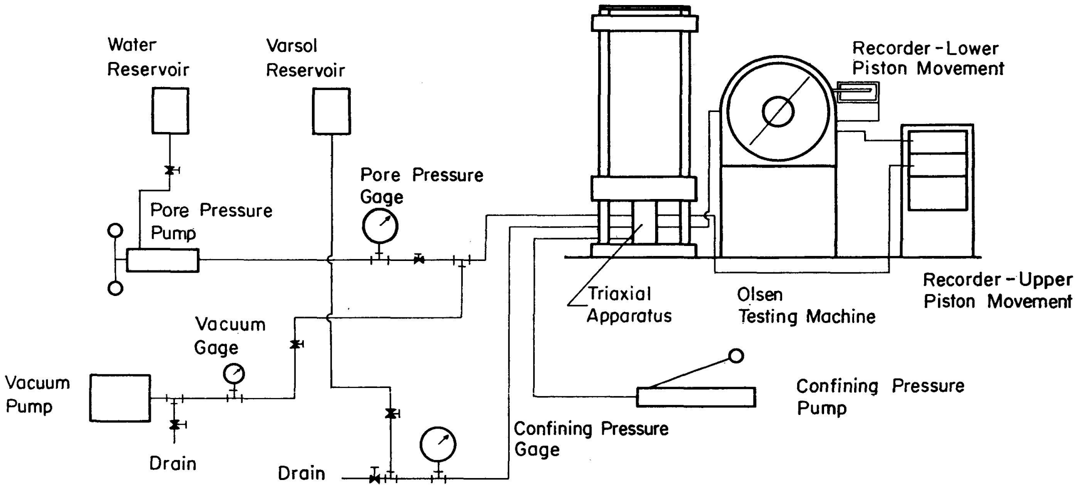

Fig. 3. Schematic diagram of test facility.

Specimens and Specimen Preparation

All the specimens used in this investigation were cored from blocks approximately $6'' \times 6'' \times 12''$ which were cast for each mixture. The cement used was Type I Portland Cement and the sand used in the mortar mix was 40—60 Ottawa Sand. All proportions shown are by weight, including the water-cement ratio. The proportions and water-cement ratios for the mortar specimens are shown in Table 1. The neat cement cylinders were cored from blocks which were cast with a water-cement ratio of 0.40 and mechanically vibrated.

A commercial diamond core drill using water as a lubricant was rotated in

Table 1. Mortar mixes tested

Mix proportions by weight	Group		Water-cement ratio	Compressive strength, psi	Tensile strength, psi
	un-jacketed	jacketed			
0.75 part portland cement 0.25 part pozzolan 0.92 part sand	C	D	0.98	4,210	420
1 part portland cement 2 parts sand	E	F	0.60	4,960	430
1 part portland cement 3 parts sand	G	H	0.88	2,910	260
1 part portland cement 1 part sand 0.64 part expanded clay aggregate	I	J	1.00	2,320	185

a drill press to core the specimens from the parent block. The specimens were then placed in a longitudinally split aluminum tube and clamped in a vise on the bed of a diamond cut-off saw. The saw had two blades spaced one inch apart and cut both ends of the specimen simultaneously. This assured uniform length specimens with smooth and parallel ends. The diameter of the specimens varied from 0.501 to 0.503 inches and the length varied from 1.002 to 1.005 inches.

Specimens were kept in water at all times during the fabrication procedure to assure uniform curing. When fabrication was completed, all of the samples were submerged in water in a vacuum dessicator for a period of three days. At this stage their wet weight was recorded. The samples were dried in an oven for three days at 105° C and cooled, then placed in a vacuum dessicator for three days. Their dry weight and dimensions were then recorded. Specimens were stored in a dessicator until ready to be tested.

The mortar specimens which were tested unjacketed were saturated prior to testing with the same oil used in the test cell. The neat cement specimens subjected to pore pressure were saturated with distilled water prior to testing. Jacketing of the specimens was done with clear vinyl tubing $^5/_8$″ O.D. × $^1/_2$″ I.D. which extended over the specimen platters in the test cell.

Test Procedure

In Fig. 2 it can be seen that the upper piston P_1 bears on a soft steel slug, which bears on the upper end of the specimen. Similarly, a soft steel slug is placed between the lower end of the specimen and the top of stopper R. At both ends of the specimen a brass sleeve was fitted over the end of the stopper (or piston), over the slug, and one-eighth inch onto the specimen. This last one-eighth inch was slotted to minimize end restraint on the specimen. The plastic jacket of vinyl tubing, when used, encased the specimen and extended from the platter on stopper R and sealed on the top piston P_1. The specimen assembly is shown in Fig. 4.

The test program consisted of the following: 1. neat cement cylinders with dry voids tested @ 0; 5,000; 10,000; 15,000; and 20,000 psi confining pressure, 2. neat cement cylinders with wet voids tested with pore pressure of 0, 20%, 40%, 60%, 80%, and 100% of the confining pressure with confining pressures of 0; 2,500; 5,000; 10,000; 15,000; and 20,000 psi. 3. mortar specimens tested jacketed (dry voids with zero pore pressure) and unjacketed (saturated with oil) at confining pressures of 0; 2,500; 5,000; 7,500; 10,000; 12,500; 15,000; and 17,500 psi. This test program encompassed 110 neat cement specimens and 202 mortar specimens. All entrapped air was carefully bled from all supply lines as each test was made in the cell. In all tests the confining pressure was applied to the specimen prior to the application of axial load.

Test Results and Interpretation

Stress vs. Strain

Fig. 5, 6, and 7 show typical stress-strain curves obtained from the cylinders that were tested. Fig. 5 shows stress-strain curves for eight of the mortar cylinders, Group H, at different confining pressures. Fig. 6 shows a similar set of curves for eight of the structural lightweight mortar cylinders, Group J. Fig. 7 shows curves for five of the neat cement cylinders tested with dry voids at different confining pressures. All curves are for jacketed specimens, and all are shown originating from the state of equal triaxial stress, which was the condition at which excess axial load was first applied.

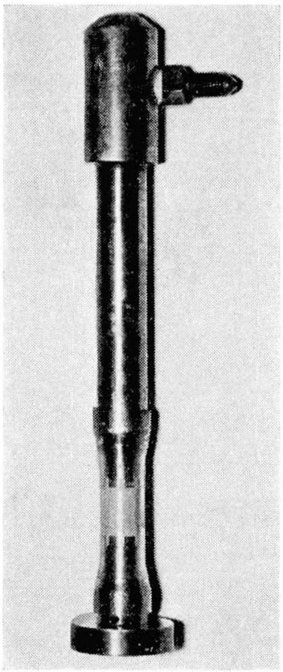

Fig. 4.

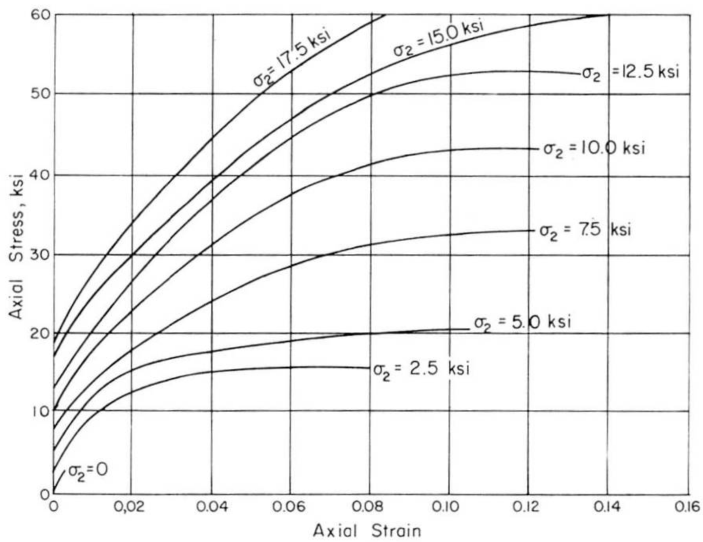

Fig. 5. Stress-strain curves, mortar group H (1 : 3 mortar, jacketed).

Features common to all three figures are readily apparent: the non-linear nature of the stress-strain relationship and the great increase in axial strength and ductility which confining pressure gives to the material.

In comparing Fig. 5 and 6, it is noted that the lightweight mortar showed greater axial strain than conventional mortar at the same stress level, most likely because of its greater porosity.

Stress vs. Volume Change

It was pointed out above that the design of the triaxial test cell made possible the measurement of total volume change of a jacketed specimen during a triaxial test. This in turn made possible a quantitative study of the volume change of such a specimen with increase in axial stress. Typical curves

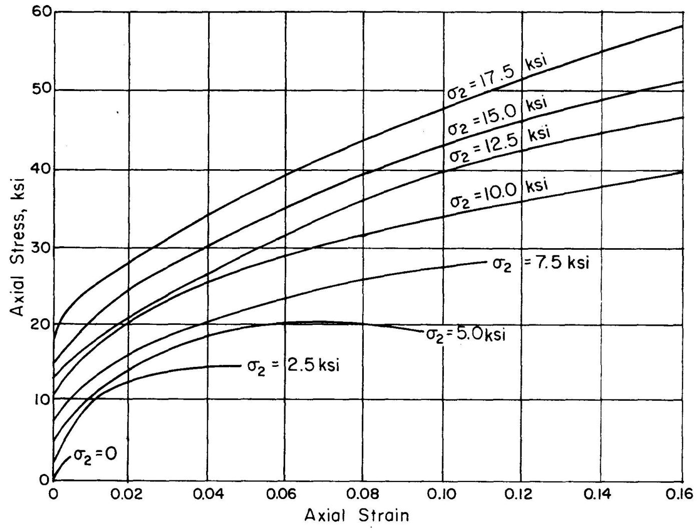

Fig. 6. Stress-strain curves, mortar group J (structural lightweight mortar, jacketed).

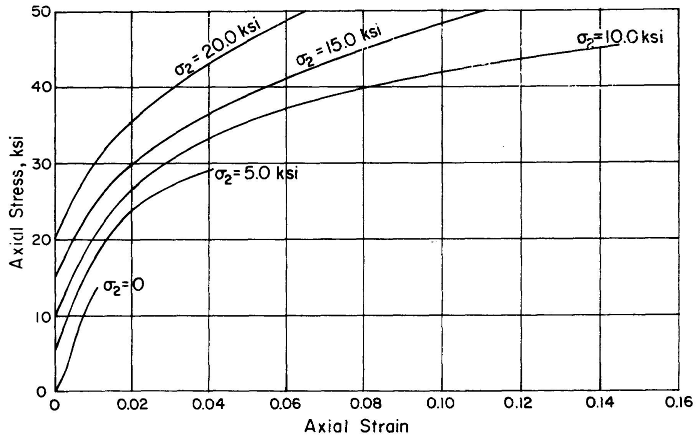

Fig. 7. Stress-strain curves, neat cement cylinders, no pore pressure, dry voids.

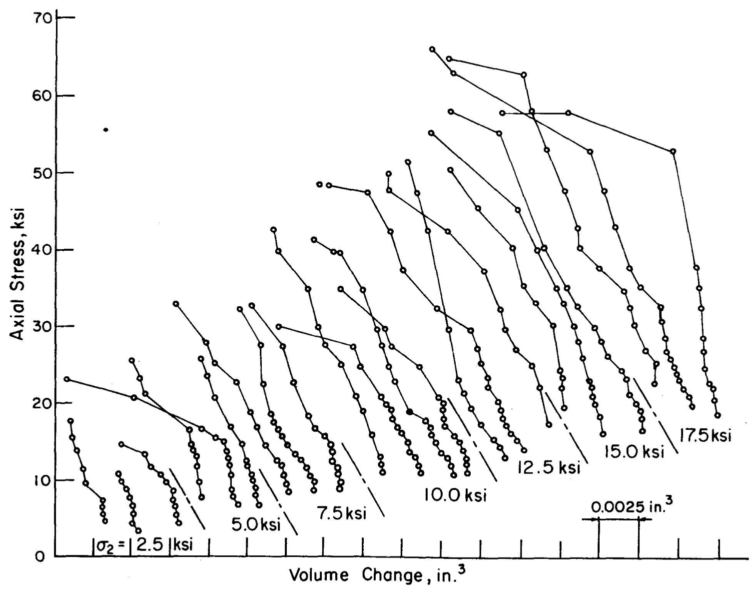

Fig. 8. Stress-volume change curves, mortar group H (1 : 3 mortar, jacketed).

of axial stress vs. volume change are shown in Fig. 8, 9, and 10. Curves for the mortar specimens of Group H are shown in Fig. 8, curves for the lightweight mortar specimens of Group J are shown in Fig. 9, while curves for neat cement specimens with dry voids are shown in Fig. 10.

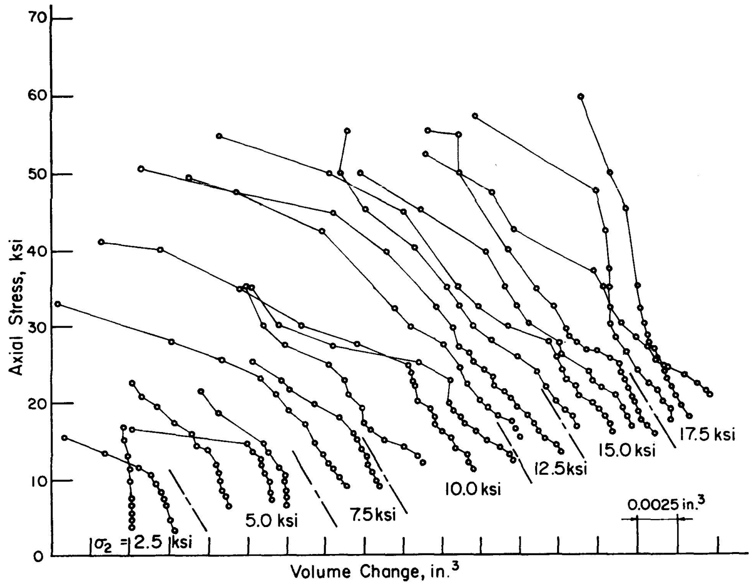

Fig. 9. Stress-volume change curves, mortar group J (structural lightweight mortar, jacketed).

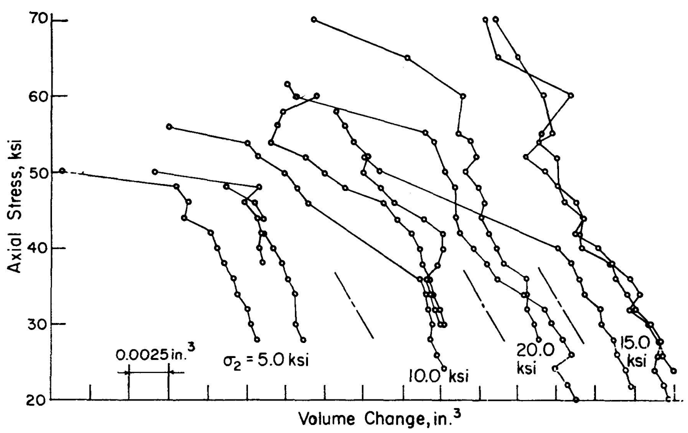

Fig. 10. Stress-volume change curves, neat cement cylinders, no pore pressure, dry voids.

Each curve in Fig. 8 and 9 is shown originating from the state of equal triaxial stress. In Fig. 10 only the upper portions of most curves are shown. In all three figures each curve is plotted from a different origin for ease of reading.

For every jacketed specimen tested, volume was found to decrease as the axial load was increased, and this was true at every stage of loading. In the figures this is reflected by the fact that each curve swings to the left, indicating negative volume change, with increasing axial stress. In comparing Fig. 8

Table 2. Summary of measured and computed values, mortar cylinders

Group	No. of specimens tested	Confining pressure psi	Measured axial strength psi	Computed axial strength psi	Empirical constants		Coefficient of correlation
					a	b	
E	3	0	5740	—	1.353	0.851	0.998
	3	2500	9690	9567			
	3	5000	12500	12647			
	3	7500	15350	15496			
	2	10000	17600	18205			
	3	12500	21000	20815			
	3	15000	23600	23347			
	3	17500	26400	25818			
C	3	0	4800	—	1.480	0.803	0.997
	3	2500	9090	9006			
	3	5000	12300	12141			
	3	7500	14700	14968			
	3	10000	16800	17611			
	3	12500	19700	20126			
	3	15000	23000	22544			
	3	17500	26000	24883			
G	3	0	3200	—	1.679	0.791	0.998
	3	2500	7700	7620			
	3	5000	10890	10851			
	2	7500	13210	13746			
	3	10000	16390	16442			
	3	12500	19300	19000			
	3	15000	21390	21452			
	3	17500	24200	23820			
I	3	0	2350	—	2.006	0.754	0.996
	3	2500	7600	7290			
	3	5000	10250	10685			
	3	7500	13120	13670			
	3	10000	16100	16416			
	3	12500	19030	18996			
	2	15000	21850	21452			
	3	17500	24750	23809			

F	5	0	5620	—	4.242	0.856	0.999
	3	2500	17700	17533			
	4	5000	27200	27191			
	3	7500	35100	36149			
	3	10000	44500	44680			
	4	12500	53500	52908			
	4	15000	61100	60902			
	4	17500	69300	68705			
D	5	0	4870	—	3.949	0.956	0.996
	3	2500	14300	15034			
	3	5000	26500	24596			
	3	7500	35000	33943			
	3	10000	43000	43153			
	3	12500	52500	52263			
	3	15000	61600	61293			
	4	17500	66500	70259			
H	5	0	3160	—	4.449	0.879	0.999
	3	2500	14300	14602			
	3	5000	24800	24205			
	3	7500	33600	33218			
	4	10000	42000	41868			
	3	12500	50900	50257			
	3	15000	58500	58444			
	3	17500	64500	66468			
J	4	0	2480	—	4.415	0.894	0.998
	3	2500	13800	13509			
	3	5000	21900	22985			
	2	7500	31600	31951			
	3	10000	41600	40602			
	3	12500	50600	49025			
	4	15000	58000	57272			
	3	17500	63400	65374			

Table 3. Summary of measured and computed values, neat cement cylinders

Group	Test number	No. of specimens tested	Confining pressure psi	Pore psessure psi	Measured axial strength psi	Computed axial strength psi	Empirical constants a	Empirical constants b	Coefficient of correlation
DRY	1-C	3	0	dry voids	13500	—	3.003	0.882	0.999
	2-C	3	5000	dry voids	30200	30384			
	3-C	3	10000	dry voids	45100	44616			
	4-C	3	15000	dry voids	58700	57994			
	5-C	3	20000	dry voids	69700	70845			
WET	26-C, 31-C	6	0	wet voids	7000	—	2.665	0.727	0.995
	32-C	3	2500	wet voids	15300	15823			
	27-C	3	5000	wet voids	22900	21609			
	28-C	3	10000	wet voids	31600	31190			
	29-C	3	15000	wet voids	39300	39489			
	30-C	3	20000	wet voids	45700	47052			
20%	33-C	3	2500	500	14900	15014	2.479	0.750	0.999
	6-C	3	5000	1000	20600	20484			
	7-C	3	10000	2000	30600	29687			
	8-C	2	15000	3000	36800	37757			
	9-C	3	20000	4000	45100	45170			

40%	34-C 10-C 11-C 12-C 13-C	3 3 3 3 3	2500 5000 10000 15000 20000	1000 2000 4000 6000 8000	13400 19300 27800 37500 43700	13580 18782 28096 36662 44775	2.233	0.840	0.998
60%	35-C 14-C 15-C 16-C 17-C	3 3 3 3 3	2500 5000 10000 15000 20000	1500 3000 6000 9000 12000	13000 17700 26100 33600 40300	13024 17684 25949 33494 40606	2.015	0.826	0.999
80%	36-C 18-C 19-C 20-C 21-C	3 3 3 3 3	2500 5000 10000 15000 20000	2000 4000 8000 12000 16000	12000 15900 23000 29300 37700	11932 15952 23249 30029 36494	1.708	0.860	0.999
100%	37-C 22-C 23-C 24-C 25-C	3 3 3 3 3	2500 5000 10000 15000 20000	2500 5000 10000 15000 20000	10700 13400 18300 24000 29500	10588 13535 18904 23906 28683	1.249	0.865	0.998

and 9, it is readily apparent that the decrease in volume of the lightweight mortar was greater than that of the conventional mortar. It is presumed that the greater volume of voids in the lightweight mortar accounts for this greater decrease in volume.

Axial Strength vs. Confining Pressure

In each triaxial test of a cylinder to failure, the axial strength was taken to be the axial stress corresponding to the greatest axial force sustained by the cylinder during the test. Table 2 summarizes the measured values of axial strength and corresponding confining pressures for all of the mortar cylinders tested. Table 3 summarizes the measured values of axial strength and corresponding confining pressures and pore pressures for all of the neat cement cylinders tested. Also, Tables 2 and 3 show correlation of the measured data with values obtained from the empirical equation

$$\left(\frac{\sigma_1}{\sigma_u}\right) = 1 + a\left(\frac{\sigma_2}{\sigma_u}\right)^b, \tag{1}$$

where
σ_1 = confined axial strength,
σ_2 = confining pressure,
σ_u = unconfined axial strength,
a, b = empirical constants.

Eq. (1) requires that

$$\log\left[\left(\frac{\sigma_1}{\sigma_u}\right) - 1\right] = \log a + b \log\left(\frac{\sigma_2}{\sigma_u}\right) \tag{2}$$

which is a linear relationship between log $[(\sigma_1/\sigma_u) - 1]$ and log (σ_2/σ_u). To determine constants a and b, data from the tests were interpreted by the method of least squares to achieve the "best" straight line for Eq. (2). The computed values of a and b are shown in Tables 2 and 3, together with corresponding values of axial strength computed by Eq. (1). As a further quantitative measure of correlation, the coefficient of correlation was calculated for each set of values a and b. The coefficient of correlation is the ratio of explained variation to total variation of the data about its mean [2]. Values of the coefficient are also shown in Tables 2 and 3.

Fig. 11 shows a non-dimensional graphical presentation of the data for axial strength vs. confining pressure for the mortar cylinders of Groups G, H, I, and J. Each data point represents the results of several tests to destruction of presumably identical specimens, usually three. The smooth curves which are shown are graphical representations of Eq. (1) using the proper values of a and b from Table 2. This figure is typical of the data from the mortar tests and clearly shows the great increase in axial strength because of confining pressure, almost independent of the type of aggregate used. Also apparent is the great difference between the strength of the jacketed and unjacketed specimens.

Fig. 12 is similar to Fig. 11 and shows results for the neat cement cylinders, which were tested under different ratios of pore pressure to confining pressure. This figure shows most markedly the increase in axial strength which confining pressure contributes, and also the diminishing of this effect as the ratio of pore pressure to confining pressure is increased.

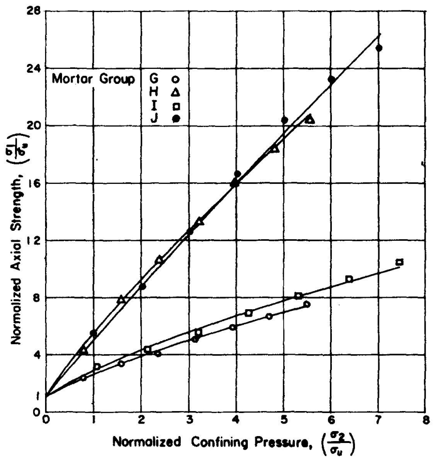

Fig. 11. Axial strength vs. confining pressure, mortar groups G, H, I, J.

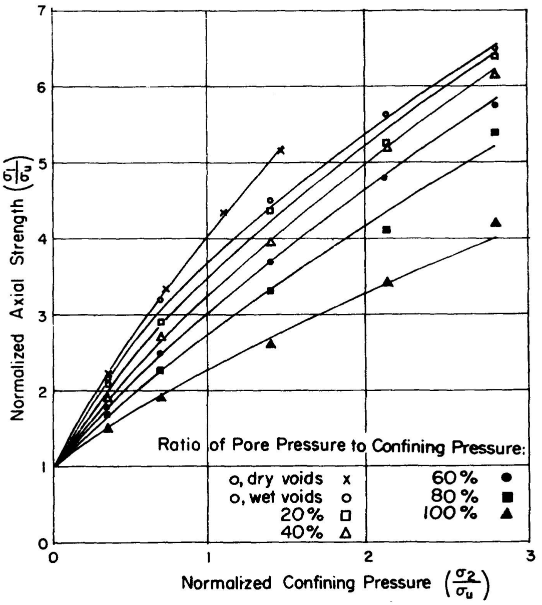

Fig. 12. Axial strength vs. confining pressure, neat cement cylinders, all groups.

Conclusions

Based on the test results and interpretation presented above, the following conclusions are offered:

1. All jacketed specimens without pore pressure, whether mortar or neat cement, showed large increases in axial strength when confining pressure was present. They also exhibited ductile behavior, taking increasing load while sustaining large strains and bulging into a barrel shape.

2. As the ratio of pore pressure to confining pressure was increased for the neat cement cylinders, the increase in axial strength due to confining pressure was diminished, but even with pore pressure equal to confining pressure, confined specimens were stronger than unconfined specimens.

3. The quantitative effect of confining pressure on axial strength of mortar or neat cement cylinders can be expressed by the empirical equation

$$\left(\frac{\sigma_1}{\sigma_u}\right) = 1 + a\left(\frac{\sigma_2}{\sigma_u}\right)^b,$$

where σ_1 = confined axial strength,
σ_2 = confining pressure,
σ_u = unconfined axial strength,
a, b = empirical constants which depend on pore pressure,

and other conditions of a particular test series. This equation seems to fit the test data very well when used with values of constants a and b determined by the methods of least squares.

4. Measurements of total volume change of jacketed specimens during the triaxial tests indicated a decrease in volume with increasing axial stress for all specimens at all stages of loading.

5. Results obtained for increase in axial strength with confining pressure seem to agree very well with those of other investigators in the range in which data overlap. This would seem to justify the use of the very small size of specimens utilized in this study, viz., a one-half inch diameter by one inch long cylinder. It is believed that careful attention to fabrication and dimensional control of the cylinders contributed to success in using such small specimens.

Acknowledgements

Testing of the mortar specimens reported in this paper was performed by Mr. Erkin Erkman and testing of the neat cement specimens was performed by Mr. Sidney P. Victory, Jr., in partial fulfillment of the requirements for their respective degrees of Master of Science in Civil Engineering at Rice University.

Bibliography

1. D. T. Griggs: "Deformation of Rocks Under High Confining Pressures." Journal of Geology, Vol. 44, 1936, p. 541—577.
2. Murray R. Spiegel: "Theory and Problems of Statistics." Schaum Publishing Co., New York, 1961, p. 359.

Summary

This paper reports the results of triaxial tests to destruction of 110 neat cement cylinders and 202 mortar cylinders. Cylinders were one-half inch diameter by one inch long and were drilled and cut to size with careful dimensional control. Several aggregates were used in the mortar specimens, including one lightweight aggregate. Each specimen was placed under constant confining pressure, then axial stress was increased to failure. Several different confining pressures were used, up to 20,000 psi, and several different ratios of pore pressure to confining pressure, and data are presented showing the influence of these factors. The effect of confining pressure, σ_2, on unconfined axial strength, σ_1, is interpreted by means of the equation $(\sigma_1/\sigma_u) = 1 + a\,(\sigma_2/\sigma_u)^b$, where σ_u is unconfined axial strength and a and b are empirical constants. Data are also presented showing axial stress vs. axial strain and axial stress vs. total volume change during the triaxial tests.

Résumé

Cet article donne un compte rendu des résultats d'essais triaxiaux menés jusqu'à la rupture de 110 éprouvettes cylindriques en ciment pur et de 202 autres constituées par du mortier. Le carottage des cylindres et leur coupe en longueur ont été l'objet d'un contrôle dimensionnel minutieux; longs de 1 pouce (2,54 cm), ces cylindres avaient un diamètre de $^1/_2$ pouce (1,27 cm). Plusieurs agrégats ont été utilisés pour les éprouvettes en mortier, dont de l'argile gonflante. Avant d'augmenter les efforts axiaux jusqu'à la rupture, les éprouvettes ont été placées dans les conditions d'une étreinte constante. Différentes pressions d'étreinte ont été appliquées, la plus élevée étant de 1400 kg/cm^2, avec différents rapports pression interstitielle/pression d'étreinte, et les résultats présentés font ressortir l'influence de ces facteurs. L'effet de la pression d'étreinte σ_2 sur la résistance axiale sous étreinte σ_1 s'exprime au moyen de la relation: $(\sigma_1/\sigma_u) = 1 + a\,(\sigma_2/\sigma_u)^b$ dans laquelle σ_u est la résistance axiale sans étreinte et a, b sont des constantes empiriques. On donne des résultats composant les contraintes axiales aux déformations axiales et à la variation de volume durant les essais triaxiaux.

Zusammenfassung

Dieser Beitrag berichtet über die Resultate dreiachsiger Versuche, bei denen 110 reine Zement- und 202 Mörtelzylinderproben zerstört wurden. Die Zylinder wurden mit kleinen Toleranzen mit einem Durchmesser von $^1/_2$ Zoll (12,7 mm) gebohrt und auf eine Länge von 1 Zoll (25,4 mm) geschnitten. Verschiedene Zuschlagstoffe, einschließlich Leichtzuschlagstoffe, wurden für die Mörtelproben verwendet. Jede Probe wurde unter konstantem, seitlichem Druck gehalten, worauf der axiale Druck bis zum Bruch der Probe gesteigert wurde. Verschiedene seitliche Drücke bis zu 1400 kg/cm^2 sowie verschiedene Verhältnisse des Porendrucks zu seitlichem Druck wurden angewendet. Die angegebenen Versuchsergebnisse zeigen den Einfluß dieser Faktoren. Der Einfluß des seitlichen Drucks σ_2 auf die einachsige axiale Festigkeit σ_1 wird durch die Beziehung $(\sigma_1/\sigma_u) = 1 + a\,(\sigma_2/\sigma_u)^b$ beschrieben, wobei σ_u die axiale Festigkeit ohne seitlichen Druck und a und b empirische Konstanten bedeuten. Zum Schluß werden noch Diagramme mit den Beziehungen axiale Spannung/axiale Dehnung und axiale Spannung/totale Volumenänderung bei den dreiachsigen Versuchen wiedergegeben.

Leere Seite
Blank page
Page vide